CHAPTER-IV

CHAPTER - IV

Studies on Fe_2O_3 Films

4.1 Introduction

4.2 Experimental

4.2.1 Film Thickness Measurement

4.2.2 Microstructure

4.2.3 Experimental Set-up for Electrical Characterization

4.2.4 Optical Characterization

4.3 Results and Discussion

References

4.1 Introduction

While evaluating Fe_2O_3 semiconductor as an important material for solar energy conversion, it is obvious to study some physical parameters such as structural, optical and electric properties of Fe_2O_3. The study provides the knowledge of grain size, crystal structure, band-gap energy, nature of optical electronic transition, situation of energy levels, electrical conduction mechanism and type of particular semiconductor. The different experimental techniques, which are used to characterise Fe_2O_3 film, are described in brief.

4.2 Experimental

This section is devoted to describe different experimental set-ups used for the study of some properties of the film.

4.2.1 Film Thickness Measurement

Thickness of the film is measured, in present investigation, by weight difference method. This method is based on the measurement of the mass of the film which is deposited on the substrates. The mass of these films was determined by using one pan semimicro-balance.

4.2.2 Microstructure

The microstructure was observed with an optical microscope (Carl, Zeiss Leitz) with amplification 160 times to the original one.

BARR. BALASAHEB KHARDEKAR LIBRARY
SHIVAJI UNIVERSITY KOLHAPUR

4.2.3 Experimental Set-up for Electrical Characterisation

a) Dark Conductivity

The d.c. electrical conductivity in the dark was measured with the help of experimental arrangement as shown in the Fig. 4.1. Two brass plates of the same size (10 cm x 5 cm x 0.5 cm) were grewed over each other at the centre of asbestos sheet and fixed with the help of a screw. To achieve uniform temperature, two heating elements of same wattage (Tony 65 Watt) were used, in parallel, in between these brass sheets. Two sample holders made up of brass, having screwing arrangement, were fixed on the top of upper brass plate. The Fe_2O_3 films of the size 2.5 cm x 0.5 cm and .2 μm to .8 μm thick were used. The press contacts to the Fe_2O_3 films were made by two copper strips which were soldered by electrical wires to provide an external electrical connection. A mica sheet was placed in between film and brass plate in order to avoid the electrical contact between them. Ohmic contact to the Fe_2O_3 was driven by painting a silver paste on the film. Thermal radiation losses were reduced by covering the whole assembly with a metal box having internal coating of asbestos sheet. Temperature of the film was measured with the help of chromal-alumel thermocouple (24 guage) which was fixed at the centre of the upper brass plate. A transister power supply unit (TPSU) Aplab was used to pass the current through the film. The potential drop across the film was measured with the help of digital multimeter (PLA - DPM - 148) and current through the film was measured with Aplab FET nanometer (TEM - 19)

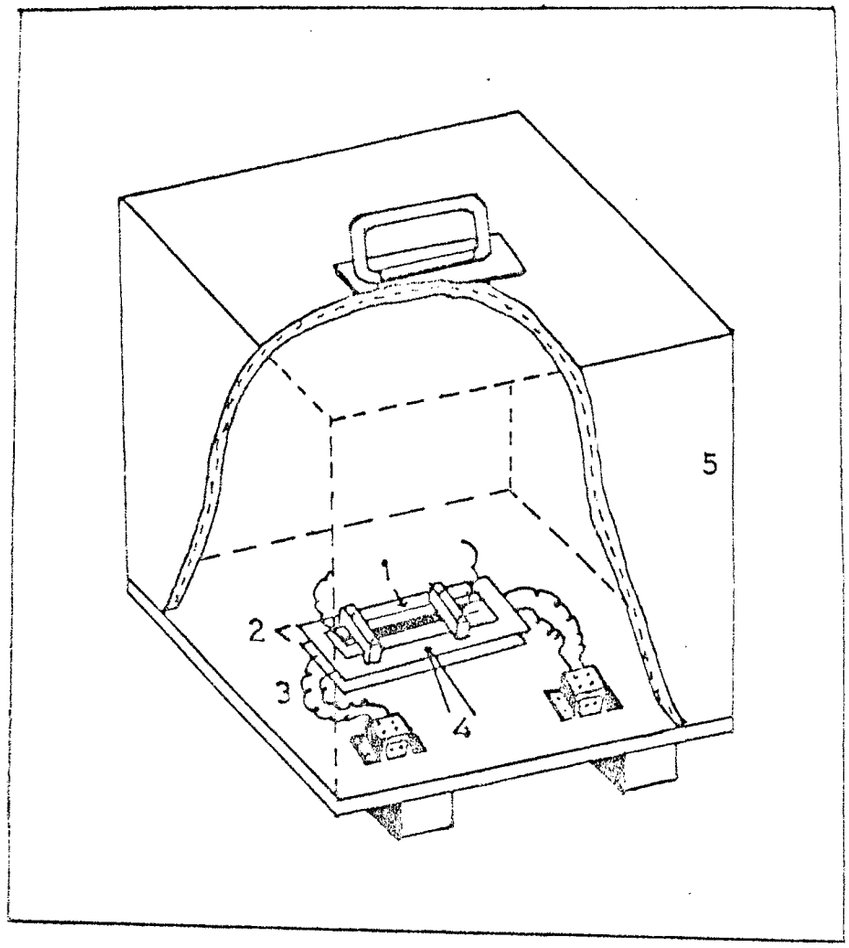

Fig.4.1 - Experimental arrangement for conductivity measurement

(1) Sample, (2) Brass plates, (3) Electrical heaters, (4) Thermocouple and (5) Shield.

b) Thermoelectric Power (TEP)

A schematic diagram for thermoelectric power (α') measurement is shown in Fig. 4.2a. A specially designed brass block was used as a sample holder-cum-heater. The typical shape of the block gives the uniform temperature gradient along the length of the sample holder. The film of the size 2.0 cm x 0.3 cm on glass substrade was used for thermoelectric power measurement. Electrical contacts to the film were made by applying silver paint and press contacts were made to it by using copper strips. Thermal gradient between the two ends of the film was established by means of two mini-heaters (H_1 and H_2) attached to the two ends of the set-up. The heaters were used not only to heat the film above room temperature but also to establish a temperature gradient-across the length of the film. Mean temperature (T) and temperature difference (ΔT) were measured with the help of Al-Cr thermocouples. The temperature gradient was measured by means of a philips D.C. microvoltmeter (P.P. 9004). Differential thermo-voltage was recorded with the help of digital D.C. Microvoltmeter (VMV 15, Vasavi Make) and mean temperature was measured with a pla-digita millivoltmeter (DPM 10) A metallic cover was used for shielding the TEP unit.

The circuit diagram of the thermoelectrical power measurement is shown in Fig. 4.2b.

4.2.4 Optical Characterisation Studies

The Fe_2O_3 films of thickness ranging between .2 μm to .3 μm and cut into size 2.5 cm x 1 cm. were used for the optical absorp-

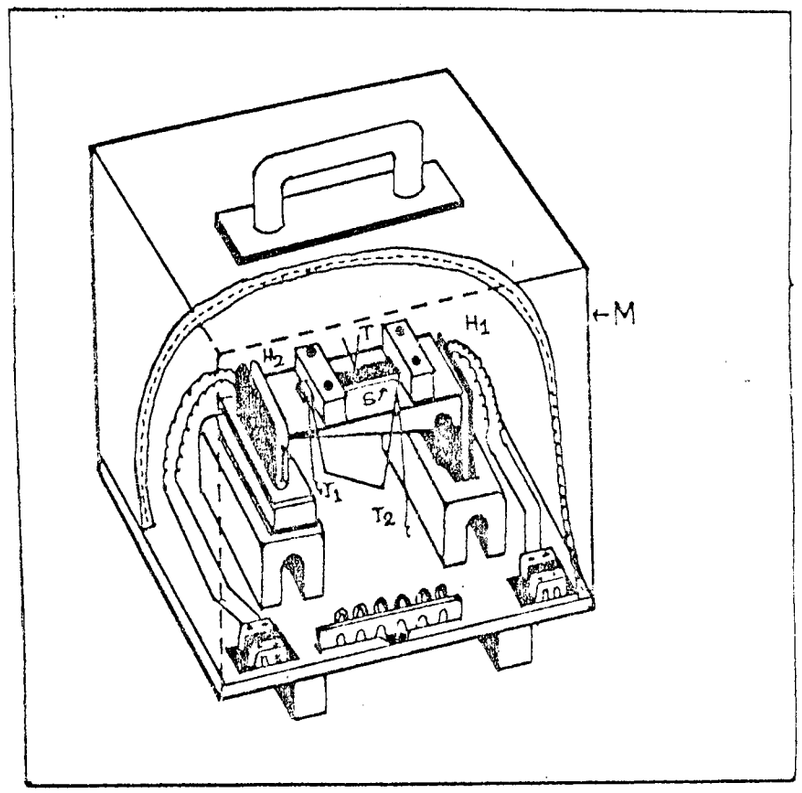

Fig. 4.2a Schematic diagram of Thermoelectric power unit. S—sample, M—metal shield, T—mean temperature thermocouple, T_1, T_2—Differential thermocouple junctions and H_1, H_2—heaters

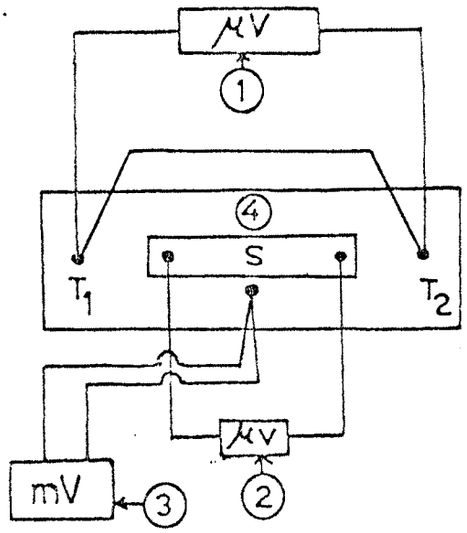

Fig. 4.2b Circuit diagram for the measureement of thermoelectric power (TEP)

1) Philips D.C. microvoltmeter
2) Digital D.C. microvoltmeter(VASAVI)
3) PLA Digital millivoltmeter
4) Sample

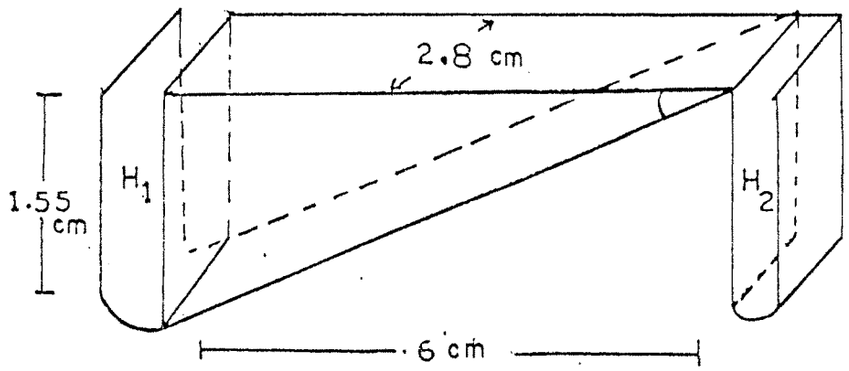

Fig. 4.2.c Design of specially mace sample holder.

tion study. The optical density (αt) was measured with a monochromator called as Spekal (Carl, Zeiss, Jena) in the wavelength range 4000 A^{o} to 8000 A^{o}.

4.3 Results and Discussion

4.3.1 Film Thickness

Thickness is one of the important parameter which determines the properties of the film. The thickness of Fe_2O_3 film was determined by weight difference method. The weight of the glass substrate before and after deposition of film were taken. The difference of these two gives mass of the Fe_2O_3 film. By knowing density of Fe_2O_3 (5.11 gms/cm^3) the thickness of Fe_2O_3 film was determined using the relation.

$$t = \frac{m}{A \times d} \quad \text{cms.}$$

where m = mass of the film in gms.

A = area of the film in cm^2

and d = density of the material of the film in gms/cm^3.

The quality of the iron-oxide films produced, using this method, depends on the concentration of the solution. The molar concentration of the $FeCl_3$ solution was varied from .02 to 2 and iron-oxide films were formed. The variation of film thickness with the solution concentration is shown in the Fig. 4.3. In the moderate concentration range (i.e. .02 M to 1.5 M) the film thickness increases with increasing molar concentration. The films formed at

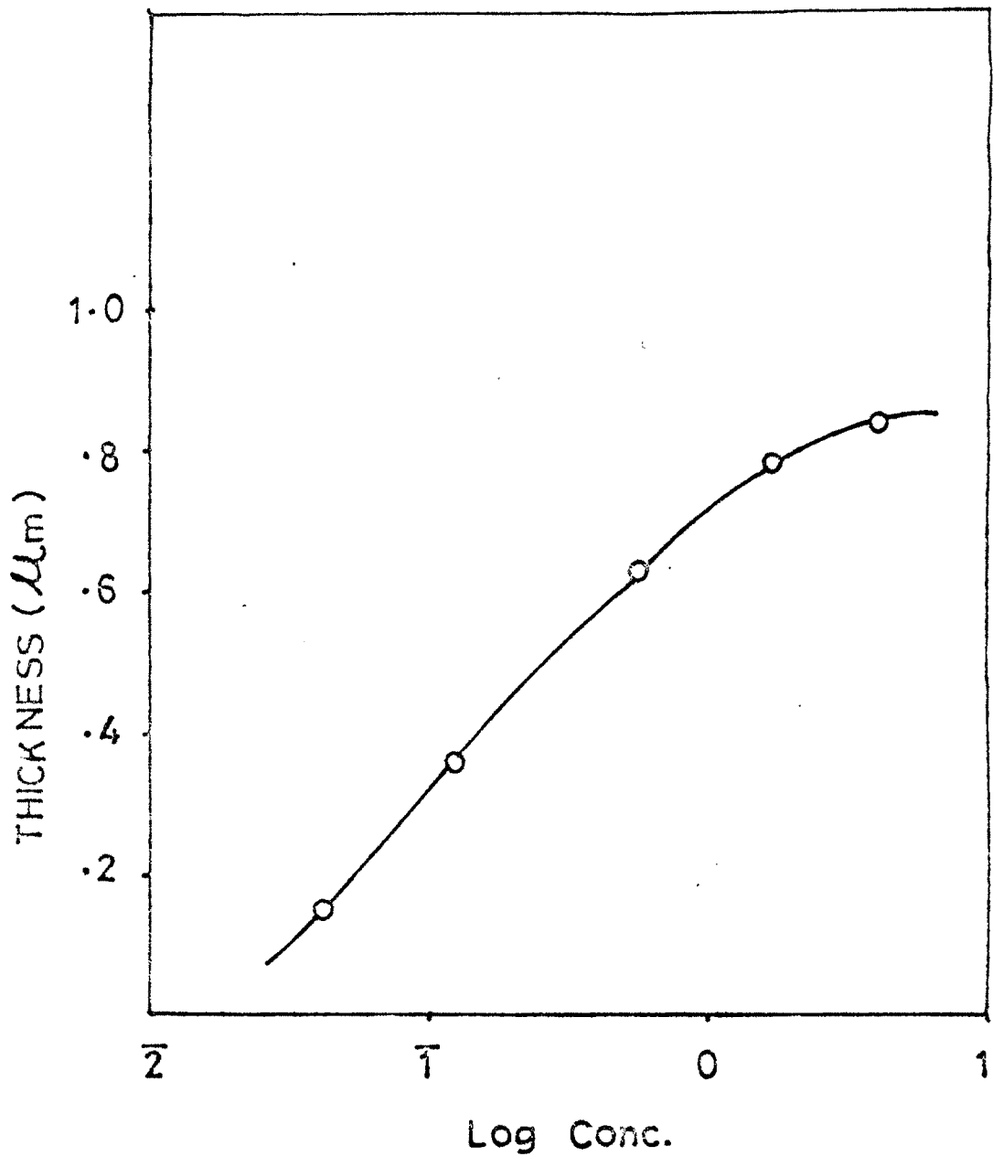

Fig. 4.3 : Variation of thickness with concentration.

lower concentration (less than .02 M) were so thin that they could not be lifted and supported on the substrate. Further pin holes and discontinuties were observed at lower concentrations. The films formed at higher solution concentrations (more than 2 M) were thicker and consisted of loss powdery precipitated particles.

4.3.2 Microstructure

The surface of the semiconductor photoelectrode has considerable influence on the characterisation of the solar cell. Microstructure study provides the information about the crystal structure of the material. The Fe_2O_3 thin films were used for microstructure study. The microstructure was observed with an optical microscope (Carl, Zeiss, Leitz Microscope) with amplification of 160 times to the original one.

From the micrograph it is seen that for concentration range .5 M to 1.5 M films are uniform and smooth, having relatively smaller grain size. For the films formed at lower concentrations crackes all over the films are observed.

4.3.3 Electrical Conductivity in Dark

Electrical conductivity is the reciprocal of electrical resistivity. The dark electrical resistivity measurement were carried out in the temperature interval between 300 ^{o}K and 600 ^{o}K. It is seen that resistance of the Fe_2O_3 film decreases with increase in temperature, which confirm that Fe_2O_3 is a semiconducting material. The plot of log R versus reciprocal of temperature is shown in Fig. 4.5.

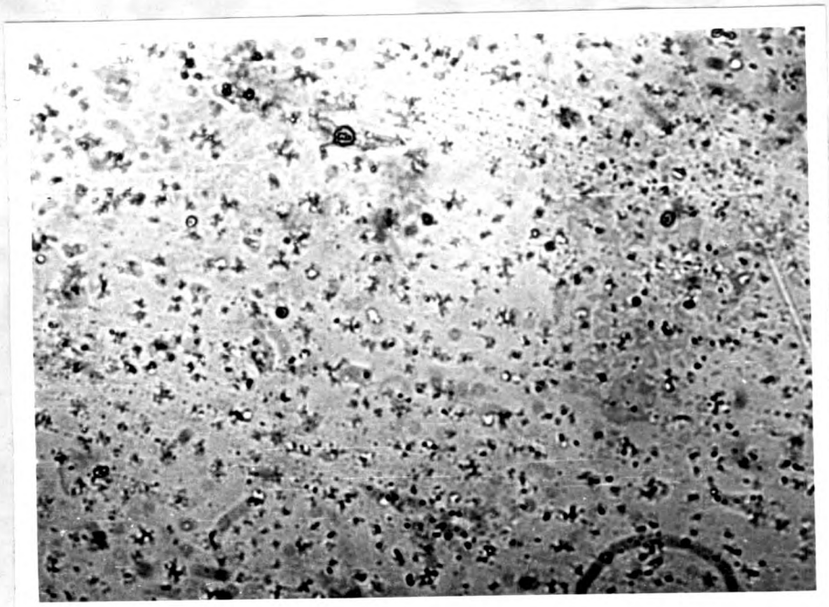

(a)

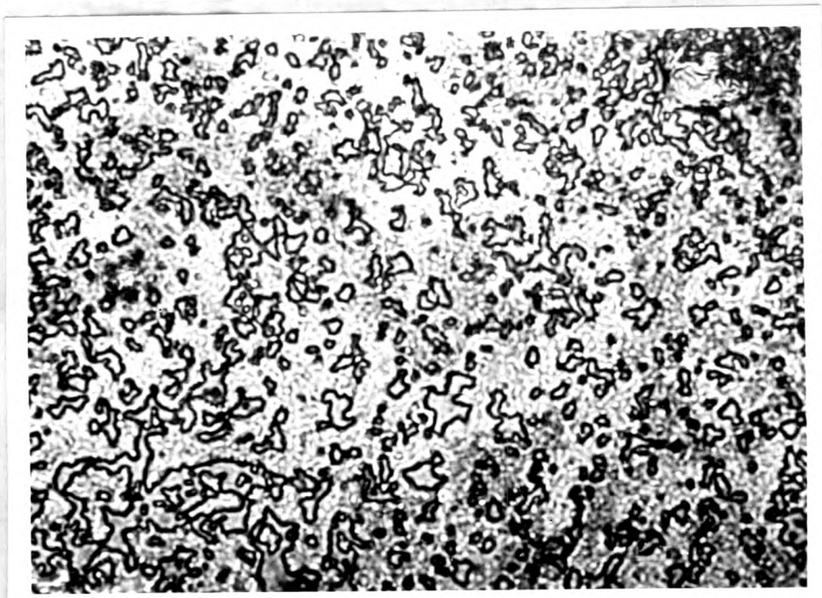

(b)

Fig. 4.4 Microstructure of Fe_2O_3 at Concentrations

(a) .05 M

(b) 2 M

SHIVAJI UNIVERSITY LIBRARY KOLHAPUR

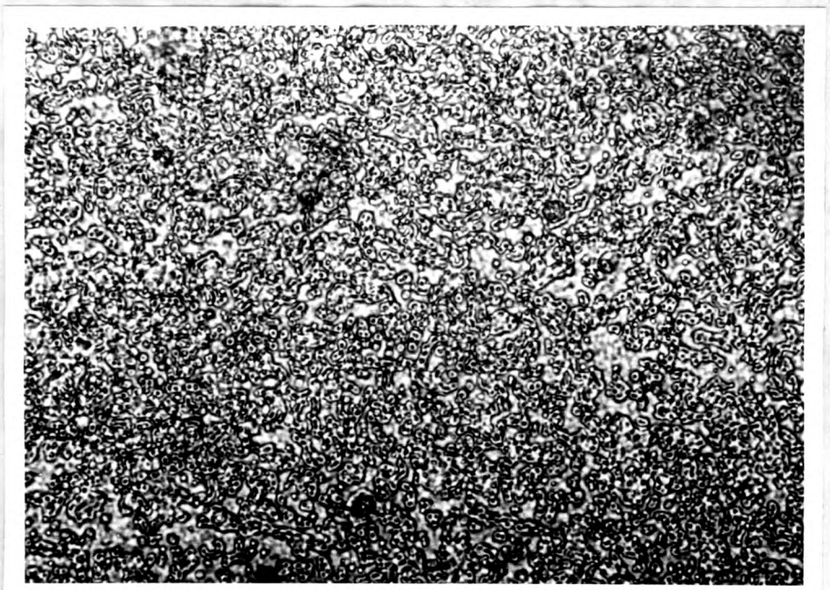

(c)

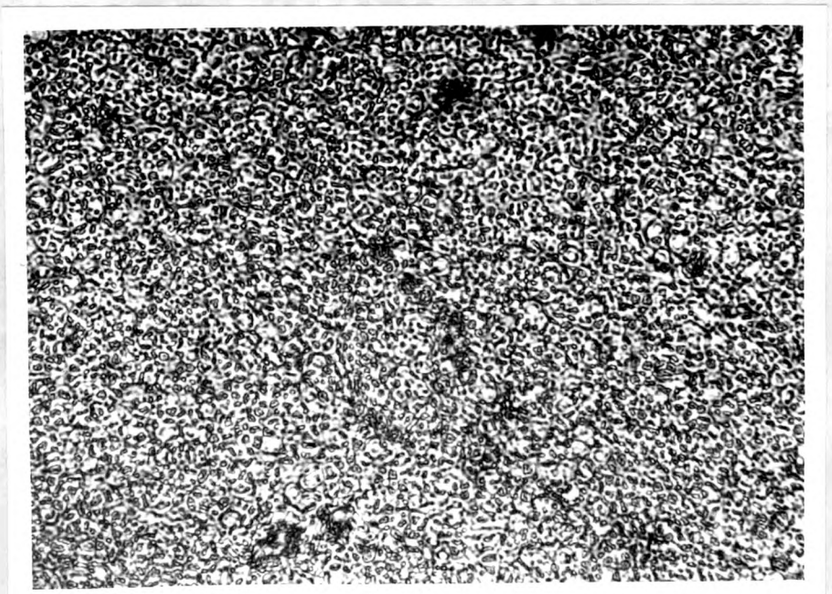

(d)

Fig. 4.4 Microstructure of Fe_2O_3 at Concentrations

(c) .5 M

(d) 1 M

The nature of plot is linear and obayes the relation /1/.

$$R = Ro \exp\left(\frac{\Delta E}{KT}\right) \quad \text{---------- } 4.3.3$$

where Ro = a constant in ohm-cm and it is the resistivity of the material at room temperature.

K = Boltzmann Constant in volts per degree

T = Temperature in ^{o}K

and E = Activation energy in eV.

The slope of the graph in Fig. 4.5 gives value of $\Delta E/K$. This graph shows clearly two different regions in the log R versus $\frac{1}{T}$ curve, namely, high temperature region and low temperature region, corresponding to the two values of the activation energies (ΔE). In high temperature region the variation of R (i.e. resistance of Fe_2O_3 film) is rapid as compared to that in the low temperature region. This can be attributed to the fact that at higher temperature the thermal energy is sufficiently high to creat vacancies which are responsible for the motion of charge carriers. On the other hand at lower temperature, thermal energy is large enough only to allow the migration of charge carriers into vacancies, already present in the material. This contributes to the constant variation of Log R with reciprocal of temperature as shown in Fig. 4.5

The observed value of activation energy in the high temperature region is .9 eV, which is slightly higher than reported by the others in this region /2-3/. The higher activation energy of Fe_2O_3 obtained may be due to higher resistance of the Fe_2O_3 film

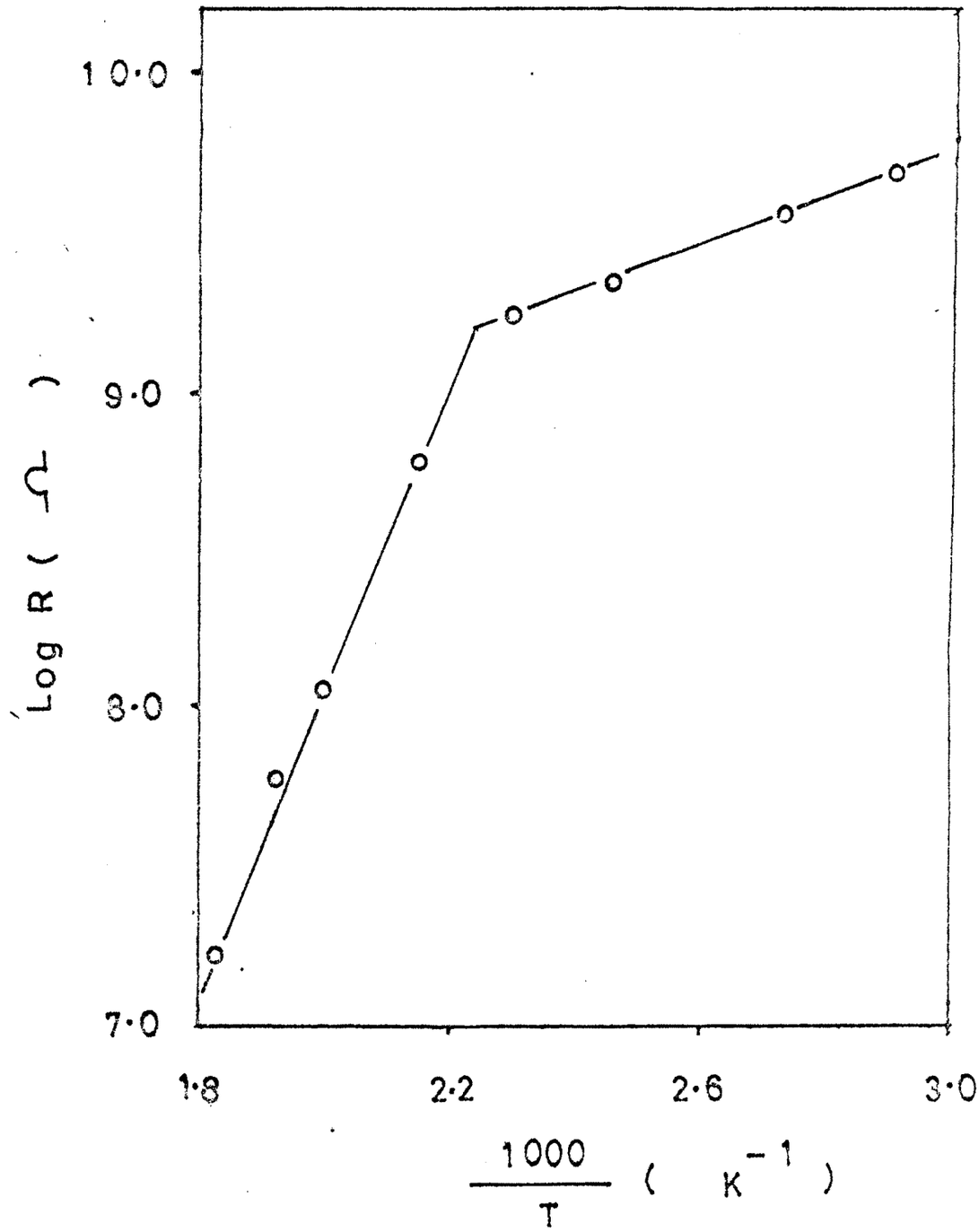

Fig. 4.5 : Plot of Log R versus reciprocal of temperature.

caused by the small grain size, because the value of ΔE is larger for the specimens of small grain size /4/. The tendency of n-type oxides to adsorb oxygen at grain boundaries is well known and the resultant increase in resistance has been studied by MORIN /5/ and SUCHET /6/ using a.c. methods. High activation energy, therefore, may be due to adsorbed oxygen at the grain boundaries of the Fe_2O_3 film. Further evidence for an accompanying increase in the activation energy for conduction is provided by the increase of temperature coefficient of resistivity /7/ resulting from the porisity in the polycrystalline specimen of n-type Ferric Oxyde.

The effect of thickness of the film on the electrical conductivity was also studied. It is seen that the conductivity increases with the thickness of Fe_2O_3 film. The increase in electrical conductivity with the film thickness can be attributed to the improved grain structure of the film /8/.

At higher temperature fast increase in conductivity is observed, which can be attributed to the fact that at higher temperature jumping of electron from one Fe site to another taking place. It is reported that when the bands are narrow and localized states are present the conduction may occur due to hopping mechanism /5,9-10/ The activation energy of .9 eV can then be considered to be the activation energy required for hopping.

4.3.4 Thermoelectric Power

The thermoelectric power α' is defined as the ratio of thermally generated voltage to the temperature difference across a

semiconductor. It is expressed by the relation

$$\alpha' = \frac{\Delta V}{\Delta T} \quad \text{----------} \qquad 4.3.3a$$

It is also known as Seebeck coefficient. The temperature difference cause a migration of the majority charge carriers. In the steady state an electric field is established which gives rise to an open circuit voltage called thermoelectric voltage, proportional to the temperature difference across the semiconductor.

The thermoelectric power is related to the density of majority charge carriers in the semiconductor. The thermoelectric power α' varies according to the relation

$$\alpha' = - \frac{K}{q} \quad A + \ln \frac{2(2me^{*} KT)^{3/2}}{nh^{3}} \qquad 4.3.3b$$

where

q = electronic charge

h = plank's constant

A = the thermoelectric factor introduced by the kinetic energy of electrons and hence dependence of scattering processes.

n = carrier concentration

M^{*}_{e} = effective mass of an electron

and K = Boltzmann constant

T = Temperature in ^{o}K

The thermoelectric power measurement were carried out in the temperature range between 300 ^{o}K and 500 ^{o}K for Fe_2O_3 films. The variation of α' with temperature is shown in Fig. 4.6. The polarity of the generated thermovoltage is negative towards the hot end of the sample. Thermoelectric power for Fe_2O_3 is of the order of microvolts.

Thermoelectric power studies shows that the electrons make dominent contribution to the conduction process, which indicate that Fe_2O_3 is n-type semiconductor. The thermoelectric power increases with temperature. The increase in α' originates due to the increase in the concentration and mobility of the charge carriers with a rise in temperature.

Most of the literature on conductivity and thermoelectric power have been predicted that conduction mechanism in oxide-semiconductors could not be interpreted in terms of assumptions of simple band theory of semiconductors. Therefore two alternative models have been put forth to explain conduction phenomena in these semiconductors. First model is concerned with the transition between 'd' levels of Fe ions. This was consistent with low mobility carriers and fit quantitatively with the data. Since Ferric-Oxide is metal excess or oxygen deficient oxide, the probability of transfer of electron from metal to metal is more. Another model involves Sp to Sp excitation as shown in Fig. 4.7. Since this model is concerned with the transfer of electron from oxygen ion to oxygen ion, it is assumed to be unfit for Fe_2O_3 in this investigation.

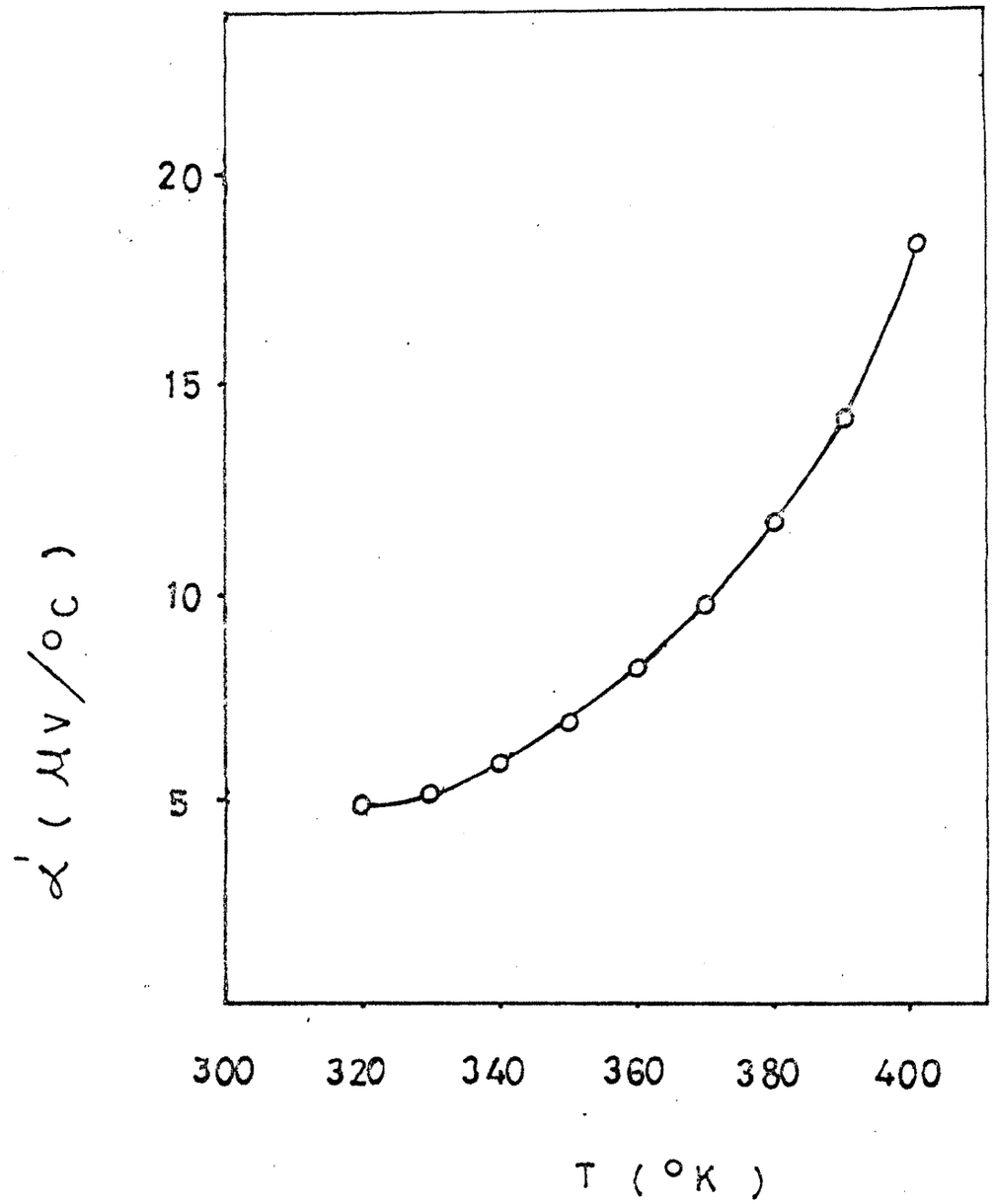

Fig. 4.6 : Plot of TEP (α') versus temperature.

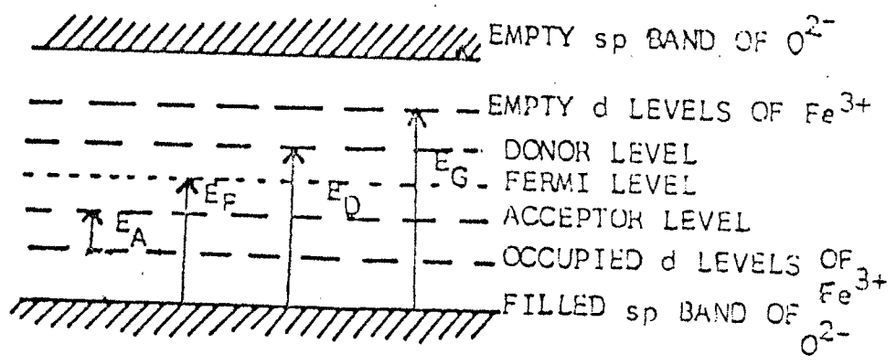

Fig. 4.7 Energy level scheme assumed in the analysis of conductivity and thermoelectric power data.

4.3.5 Optical Absorption

This study provides the information of the type of transition and the band-gap energy of the semiconductor.

The Fe_2O_3 films (having thickness .2 μm to .8 μm) and cut in to size 2.5 cm x 1 cm were used for the optical absorption study. The optical density (αt) was measured with a monochromator called as Spekal (Carl, Zeiss, Jena) in the wavelength range 4000 A^o to 8000 A^o.

In the fundamental absorption electron is excited from valance band to conduction band with absorption of a photon of energy equal to Eg, the energy of the forbidden gap. The absorption coefficient ' α ' depends on the wavelength of photon incident on the semiconductor material. The wavelength λ_e and frequency νe corresponding to the fundamental absorption edge are given by the relation

$$E_g^{op} = h\nu e = \frac{hc}{\lambda_e} \qquad \text{----------4.3.4a}$$

where

E_g^{op} = Optical energy gap and it is the energy required to excite an electron from the top of valance band to the bottom of conduction band.

The variation of αt with wavelength is shown in Fig. 4.8. It is seen that the films are highly absorbent at low wavelength and show the presence of an absorption edge.

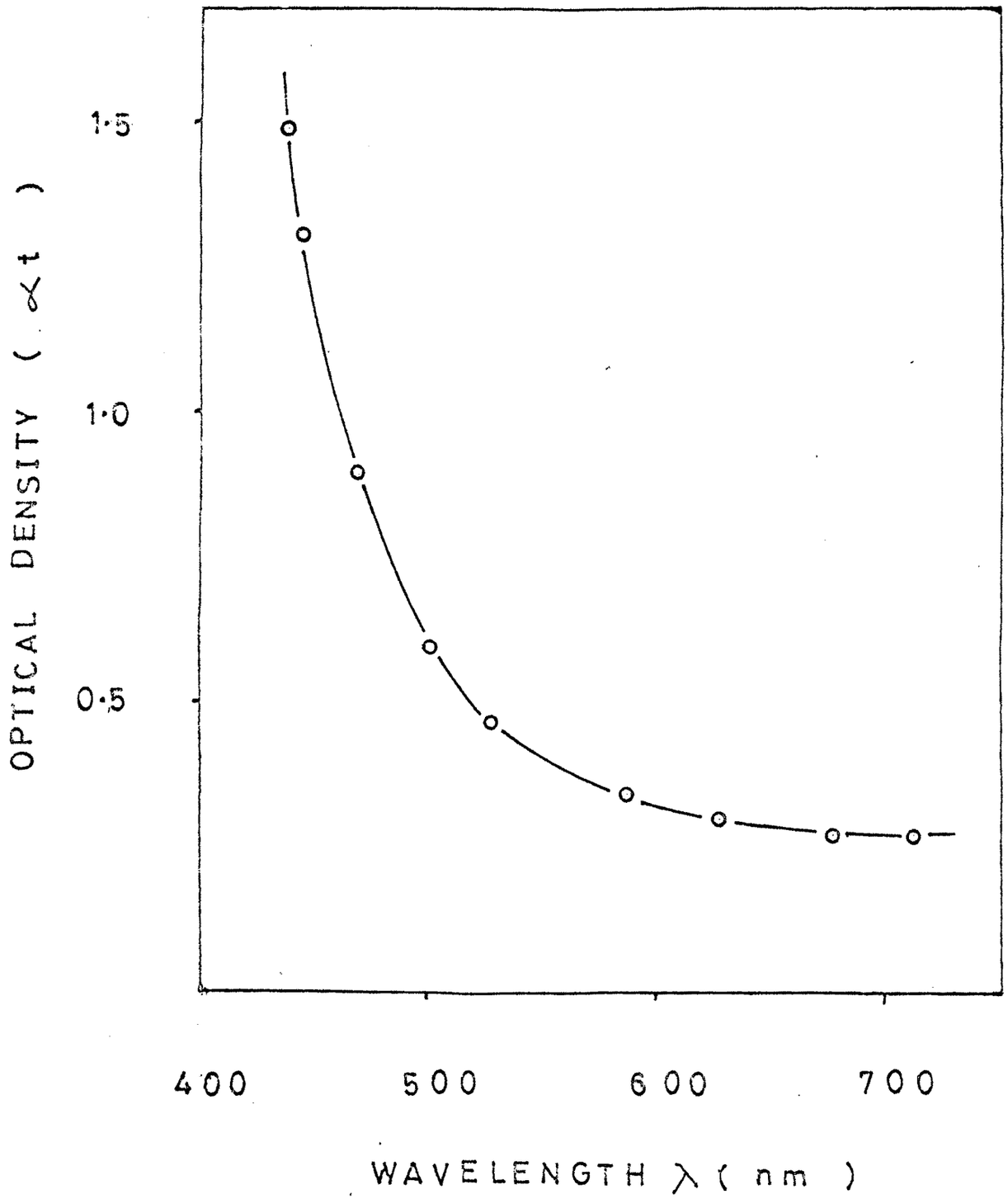

Fig. 4.8 : Plot of Optical density (∝t) versus wavelength (λ).

Semiconductors are diffrentiated into direct and indirect band-gap materials from the magnitude of absorption coeffieicnt α and its dependence on the photon energy hv. For indirect transitions the value of absorption coefficient is usually 10 to 10^3 cm^{-1}. From the optical measurements, the absorption coefficient obtained is of the order of 10^3 to 10^4 cm^{-1} in the wavelength range studied. α-Fe_2O_3 is indirect band-gap semiconductor. The large absorption coefficient obtained may be due to the overlapping of at least two absorption bands. This overlapping gives the process of charge transfer from metal to metal /11/.

In the indirect band-gap material absorption process involves an extra particle known as phonon which makes possibility of light absorption less than that of direct band-gap materials, as illustrated in Fig. 4.9. Therefore, the absorption coefficient is low and light can pass a reasonable distance into the semiconductor prior to the absorption /12/. Band-gap energy of Fe_2O_3 is determined from the plot of $(\alpha)^{\frac{1}{2}}$ versus hv, represented in Fig. 4.10. The band-gap is found to be of the order of 1.9 eV. This is in agreement with the results reported by others/13-15/.

To check the nature of the optical transitions in the sample, the graph of log (αhv) versus log (hv - Eg) has been plotted, and is shown in Fig. 4.11. The linear nature of the plot observed near the absorption edge follows the relation /16/

$$\alpha h\nu = A (h\nu - E_g)^{n'/2} \qquad \text{------ } 4.3.4b$$

where A = constant

BARR. BALASAHEB KHARDEKAR LIBRARY
SHIVAJI UNIVERSITY, KOLHAPUR.

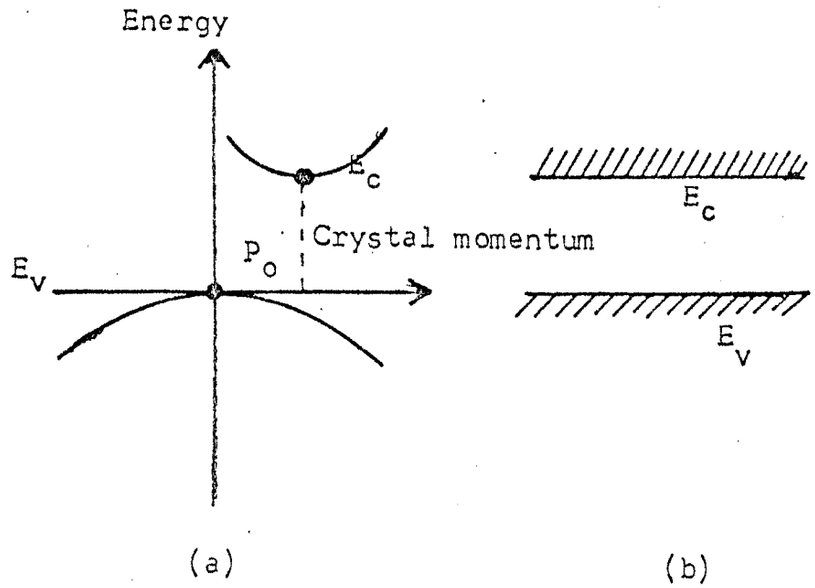

Fig.4.9.a & b : Energy crystal momentum relationships near the band edges for an indirect bandgap semiconductor.

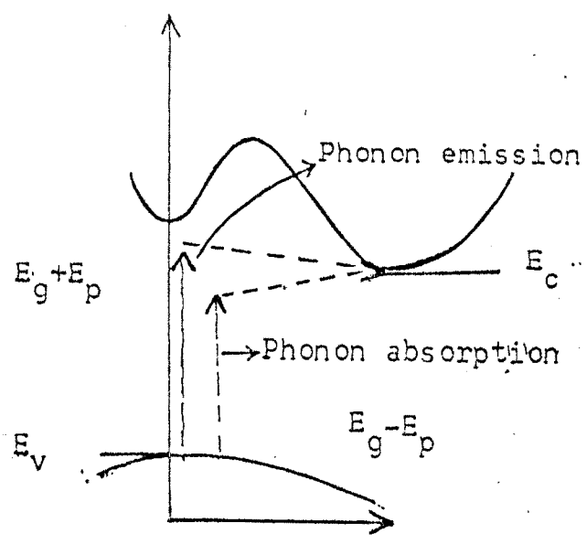

Fig.4.9.c : Energy crystal momentum diagram of an indirect bandgap semiconductor showing the absorption of photons by two step processes involving phonon emission or absorption.

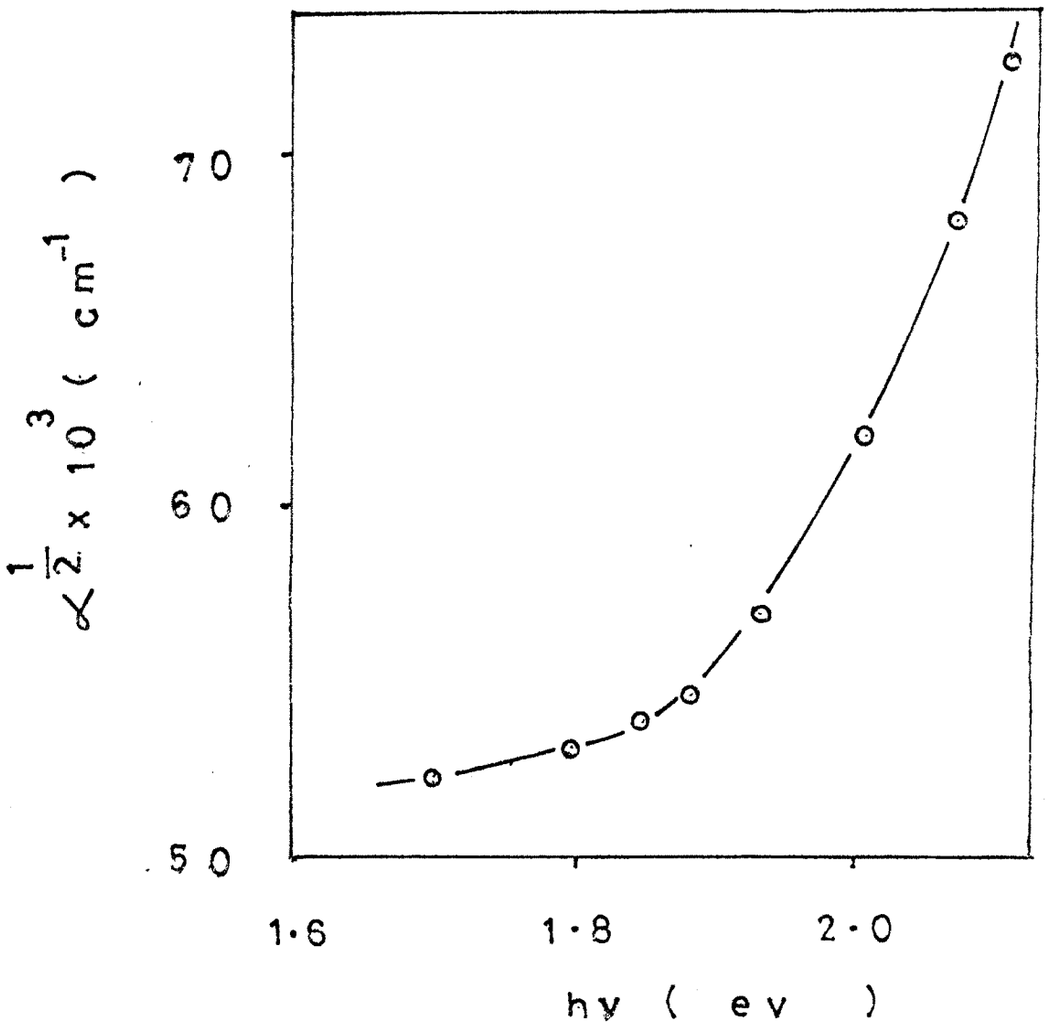

Fig. 4.10 : Plot of $\alpha^{\frac{1}{2}}$ versus hν.

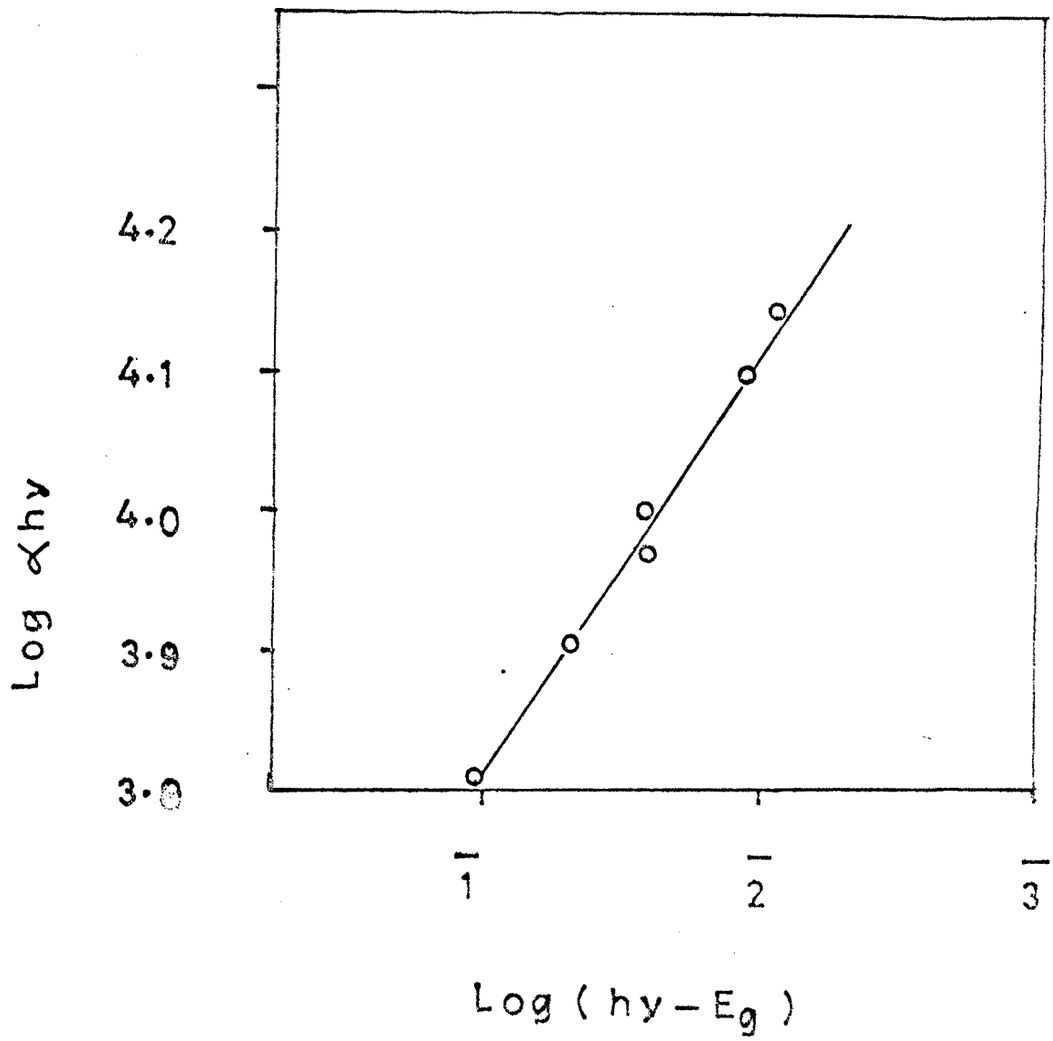

Fig. 4.11 : Plot of Log ∝hy versus Log (hy - Eg).

n' = the order which depends on the nature of transition i.e. $n' = 1$ for direct transition. and $n' = 4$ for indirect transition.

From the slope of the plot, the value of n' estimated is 4, which is in support of indirect transitions, therefore, confirming that Fe_2O_3 is the indirect band-gap material.

R E F E R E N C E S

1 L.V. Azaroff, 'Introduction to Solids' Academic Press, p. 395, (1960).

2 R.F.G. Gardner, F. Sweet and D.W. Tanner, J. Phys. Chem. Solids, Great Britain, 24, 1184, (1963).

3 S.K. Pawar and S.H. Pawar, J. Mat. Res. Bull. 18, 214, (1983).

4 R.F.G. Gardner and D.W. Tanner, Nature, Lond. 190, 1161, (1961).

5 F.J. Morin, Phys. Rev. 83, 1005, (1951).

6 J. Suchet, J. Phys. Radium, 18 , 10A, (1957).

7 P.W. Haayman, H.B. Haanstra, G.W. Hout and A. Bol, Dutch Patent (1957), Chem Abs. 52, 12630 a, (1958).

8 S.H. Pawar and P.N. Bhosale, Proc. 2nd All India Conf. on Thin Film State Phenomena', 1-6 Feb. (1984, I.I.T. Madras.

9 F.J. Morin, Phys. Rev. 93, 1195, (1954).

10 B. Roy, B.R. Chkraborthy, R. Bhattacharya and A.K. Dutta Solid State Commun., 25, 937, (1978).

11 J.H. Kennedy and K.W. Frese, J. Electrochem. Soc. 125, 709, (1978).

12 B.M. Prasad and M. Sharon Ph.D. Thesis, Bombay Univ. (1983).

13 K.S. Williem, Yun L.V. Ballenger and N. Hackerman, J. Electrochem. Soc. 126, 3, 419, (1979).

14 U. Stimming and J.W. Schutze, Ber. Bunsenges Phys. Chem. 80, 1297, (1976).

15 M.A. Branetes and L.M. Peter, J. Electroanal. Chem. 150, 593, (1983).

16 J.H. Kennedy and K.W. Frese, J. Electrochem. Soc. 125, 5, 710, (1976).